# Phase Behavior of Poly(*p*-oxybenzoate-*co*-ethylene terephthalate) (POBET): Existence of Two ET-Rich Phases

**C. L. Chung and A. C. Su***

*Institute of Materials Science and Engineering, National Sun Yat-Sen University, Kaohsiung, Taiwan 80424, R.O.C.*

**C. F. Chu***

*New Materials Research and Development, China Steel Corporation, Kaohsiung, Taiwan 81233, R.O.C.*

*Received July 8, 1994; Revised Manuscript Received December 19, 1994*®

ABSTRACT: Two glass transitions ($T_g$) located at ca. 55 and 85 °C, respectively, were identified using differential scanning calorimetry for a poly(*p*-oxybenzoate-*co*-ethylene terephthalate) (POBET) material containing ca. 55 mol % OB. The higher $T_g$ was related to the large ET-rich isotropic particles typically observed via polarized light microscopy. The lower $T_g$ was attributed to ET-rich microdomains within the continuous nematic phase, which were more fully developed after repeated thermal treatment at 300 °C. The existence of this low-$T_g$, ET-rich microphase, as confirmed by transmission electron microscopic observations, was explained in terms of precipitation of short ET-rich chains formed via transesterification within the OB-rich nematic matrix at elevated temperatures.

## Introduction

Since the pioneering work of Jackson and Kuhfuss[1] on poly(*p*-oxybenzoate-*co*-ethylene terephthalate) (POBET), numerous studies have been performed on this particular copolymer system.[1-14] It is generally accepted that, depending on the copolymer composition, POBET can be biphasic and comprised of an ET-rich isotropic phase with a glass transition ($T_g$) of ca. 80 °C and an OB-rich nematic phase with $T_g$ = ca. 170 °C.[1-7] The biphasic behavior is most clearly observable for POBET materials containing 35−80 mol % OB. This is consistent with the NMR results of Nicely et al.[8] for POBET samples of 20−80 mol % OB that compositions of the isotropic and the nematic phases are respectively ca. 35 and 80 mol % OB, independent of the bulk composition.

However, hints of further complications do exist, especially for POBET samples with ca. 60 mol % OB (POBET6). Gedde et al.[9] made a careful dielectric study of POBET6 from −180 up to +120 °C (beyond which strong space-charge effects began to set in) using a frequency range of $10^0$−$10^5$ Hz. They observed three loss peaks around +91, +64, and −50 °C at 50 Hz; they also identified a higher $T_g$ in the range of 150−160 °C (depending on the thermal history) by means of differential scanning calorimetry (DSC), which should correspond to the OB-rich nematic phase. The peak near −50 °C showed a close resemblance to the $\beta$-relaxation of ET homopolymer (PET) regarding the apparent activation energy ($E_a$ = 13 kcal/mol) and the peak width.[10] In view of the strong frequency dependence of the transition temperatures (although the corresponding $E_a$ values were not explicitly reported), the first two relaxations were assigned to two separate $T_g$'s and were taken as an indication for the presence of two different ET-rich isotropic phases. Without further delineations, Gedde et al.[9] proposed that the difference between two ET-rich phases could be due to the difference in confinement.

Benson and Lewis[11] made dynamic mechanical measurements from 1.1 to 110 Hz for POBET samples with compositions ranging from 50 to 80 mol % OB over a temperature range of 20−200 °C. For the sake of brevity, only the more prominant relaxations are recapitulated here. For POBET6, loss peaks located at 88 and 62 °C (two clear peaks, the former being stronger) with $E_a$ = 120 and 170 kcal/mol, respectively, were identified. The peak temperatures of these relaxations are in good agreement with the dielectric results of Gedde et al.,[9] and the high $E_a$ values clearly indicate that these loss peaks correspond to glass transitions.

The coexistence of isotropic and nematic phases in undiluted liquid-crystalline polymers has been explained in terms of the polydispersity effect.[15-17] On the other hand, Joseph et al.[4] have explicitly proposed that the biphasic nature of POBET is a result of the nonrandom copolymer structure; the possibility of nonrandomness in sequence distribution has in fact been repeatedly suggested by different researchers on various occasions.[12-14] The coexistence of two different ET-rich phases and a nematic OB-rich phase in POBET6, if confirmed, can have significant implications in the fundamental understanding for the phase separation phenomenon in POBET. As concisely reviewed by Sun and Porter,[7] literature conclusions concerning phase transitions in POBET6 are ambiguous or even conflicting. This certainly results from the complex nature of the system, including the biphasic nature and the possibility of ester-exchange reactions.[15-17] We suspect that the possible existence of a second ET-rich phase, which has received little attention after being first suggested by Gedde et al.,[9] may have also contributed to the confusion. Reported here are our recent observations using DSC, polarized light microscopy (PLM), and transmission electron microscopy (TEM) on the phase separation and especially the coexistence of two ET-rich phases for a POBET material comprising ca. 55 mol % OB.

## Experimental Section

**Materials.** At a molar feed ratio of OB/ET = 6/4, POBET was synthesized using the transesterification method of

* To whom correspondence should be addressed.

® Abstract published in *Advance ACS Abstracts,* August 15, 1995.

0024-9297/95/2228-7121$09.00/0 

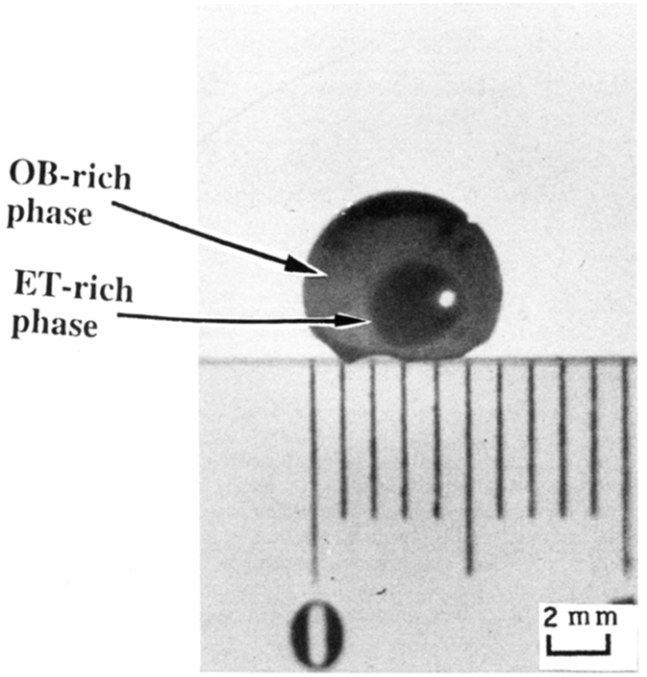


**Figure 1.** Macroscopic particle of the isotropic phase after repeated melting, pressing, and folding of the thin POBET sheet.

Jackson and Kuhfuss[1] with a slight modification that a metallic catalyst, antimony oxide in the amount of 1 wt %, was added to accelerate the ester-exchange reaction. The reaction temperature was ca. 275 °C. Mechanical stirring was maintained throughout the reaction period of ca. 3 h, after which the melt was quickly dumped from the reaction vessel onto a sheet of aluminum foil placed on top of a steel plate. In addition to acetic acid, the condensation byproduct, there was always some loss of reacting species (presumably *p*-acetoxybenzoic acid) in the form of a white powder adhering to the condenser wall during the reaction period. The as-synthesized material was dried at 110 °C for 36 h in an air-circulating oven (to remove absorbed moisture) and then stored in a desiccator before the subsequent characterization.

**Macroscopic Sample of the Isotropic Phase.** Upon elevation of temperature beyond 240 °C, the as-synthesized POBET sample (AO) underwent a dramatic change in phase morphology, forming rather large domains (ca. $10^2$ $\mu$m in size, some even visible by the naked eyes) of the isotropic ET-rich phase. Details of this process are described in the Results. Taking advantage of the viscosity difference between the isotropic and the nematic phases and the strong tendency of domains of the isotropic phase to coalesce, we were able to prepare thin disks containing a large particle (2–3 mm in diameter; cf. Figure 1) of the isotropic phase. These were obtained by heating (on a hot stage set at 300 °C) and pressing (using a sheet of polyimide release film, to "drain" the nematic liquid between domains of the isotropic phase for enhanced coalescence) of specimens, followed by quick cooling in a stream of air and folding of the thin specimens to bring regions concentrated in isotropic domains in contact. The process was typically repeated 2–3 times which corresponded to a cumulative time of approximately 2 min at 300 °C. The large particle was then cut off from the thin disk and studied separately to identify thermal behavior of the corresponding isotropic phase.

**Differential Scanning Calorimetry (DSC).** A routinely calibrated differential scanning calorimeter (Perkin-Elmer DSC7) equipped with an ice bath and liquid-nitrogen cooling accessories was used. The carrier gas was nitrogen at a flow rate of ca. 20 mL/min. Samples (typically ca. 7 mg in weight) were sealed in hermetic pans and subjected to a thermal treatment of 2 min at 300 °C (hereafter referred to as the routine thermal erasing procedure, RTEP) for the purpose of erasing earlier thermal history. This was followed by fast cooling (at a nominal rate of −200 °C/min, but the actual rate was ca. −160 °C/min near 300 °C and ca. −100 °C/min in the vicinity of 150 °C) to and isothermal annealing at a predetermined temperature ($T_a$) for a given period of time ($t_a$). The annealed sample was then quickly cooled (again at a nominal rate of −200 °C/min) to 5 °C (or, in limited cases, to −50 °C using an effluent stream of evaporated liquid nitrogen) and subsequently scanned at a heating rate of 20 °C/min up to 300 °C. On several occasions where quenching was required, samples were quickly removed from the DSC cell right after RTEP and thrown into a flask containing liquid nitrogen. These were referred to as the liquid nitrogen quenched samples.

**Table 1. Characteristics of the POBET Samples**

| code | thermal history | composition[a] (OB/ET, molar ratio) | preference factor,[b] m |
|---|---|---|---|
| AO[c] | as-synthesized | 0.54/0.46 | 1.09 |
| AT[d] | treated at 300 °C | 0.55/0.45 | 1.14 |
| AI[e] | treated at 300 °C | 0.37/0.63 | 1.09 |

[a] Determined by means of $^1$H-NMR. [b] Calculated from diad populations.[8] [c] As-synthesized. [d] RTEP-treated. [e] Macroscopic isotropic phase obtained from coalescence of ET-rich droplets at ca. 300 °C.

**Nuclear Resonance Spectroscopy (NMR).** The as-synthesized material (AO), an RTEP-treated (AT) sample, and the macroscopic isotropic phase (AI) were analyzed by use of solution $^1$H-NMR. The samples were dissolved in deuterated trifluoroacetic acid at ambient temperature. A 300-MHz nuclear magnetic resonance spectrometer (Varian VXR-300/51) was then used to determine the composition and the diad populations according to the procedure of Nicely et al.[8] Results are summarized in Table 1.

**Polarized Light Microscopy (PLM).** A polarized light microscope (Nikon OPTIPHOT-POL) equipped with a heating stage (Linkam THMS-600), a temperature control system (Linkam TMS-91), and a videorecording system (Sony DXC-755) was used. Specimens were prepared by melting of the as-synthesized sample on a glass slide on top of the heating stage at ca. 220 °C, followed by pressing of the melt with a piece of cover glass and quick cooling of the specimens in a stream of air. In limited cases, liquid nitrogen quenched (after RTEP) samples were prepared in a manner similar to those in the DSC study. Polarized light microscopic observations were then made using temperature histories approximately parallel to those in the DSC analysis to facilitate comparison.

**Transmission Electron Microscopy (TEM).** An as-synthesized POBET sample was melted in an aluminum vessel sitting on top of a hot stage at 300 °C for ca. 2 min (thus rendering it an AT sample) and then fast-cooled to ambient temperature with the vessel remaining stationary. This eliminated possible effects on microphase morphology from shear flow. The AT sample was then ultramicrotomed into specimens ca. 45 nm in thickness which were stained by use of a freshly prepared (via codissolution of $NaIO_4$ and $RuO_2$)[18] 1% aqueous solution of $RuO_4$, followed by water washing and air-drying, and then examined using a JEOL JEM-100S transmission electron microscope within an accelerating voltage range of 40–60 kV.

## Results

**Morphology Development during the First Heating.** Given in Figure 2 are the morphological changes observed during the first heating (at 80 °C/min) of the as-synthesized sample to 300 °C. Initially (cf. Figure 2a), the sample appeared only slightly heterogeneous. There were no appreciable changes in either phase mobility or morphology below 200 °C (Figure 2b, taken at ca. 85 °C). As the temperature exceeded ca. 250 °C parts c and d of Figure 2, taken at 250 and 265 °C, respectively), the nematic matrix became somewhat mobile and blurred regions of lower brightness started to appear, developing into domains (ca. 30 $\mu$m in diameter) of fuzzy boundaries, within which there were

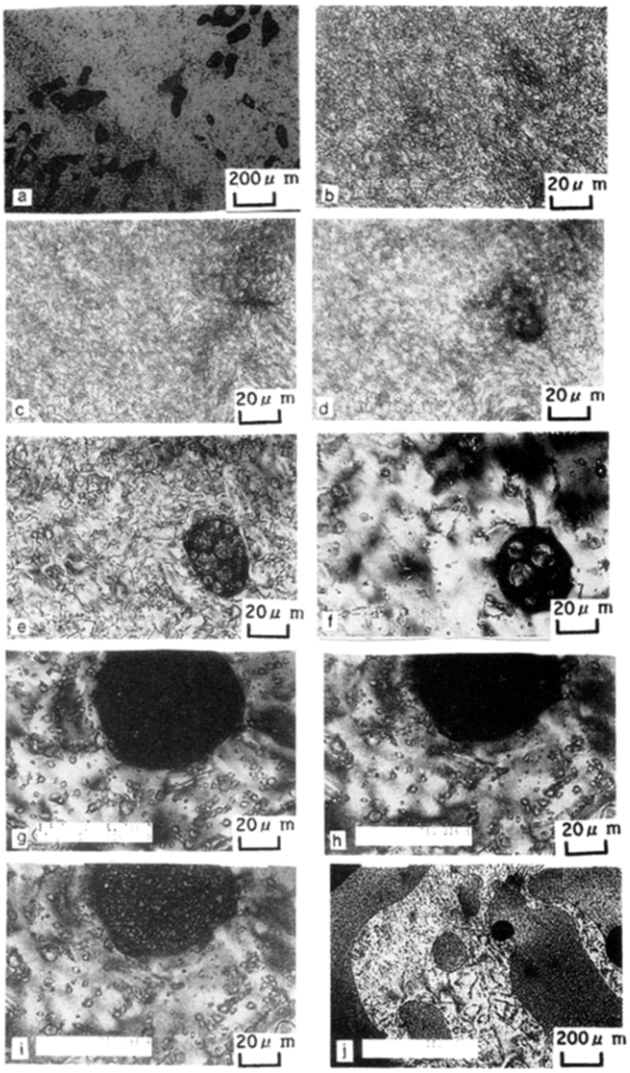


**Figure 2.** Morphological evolution (as observed via PLM) during the first heating to 300 °C and the subsequent fast cooling: (a) as-prepared specimen, room temperature; (b) heated (ca. 80 °C/min) to 85 °C; (c) 250 °C; (d) 265 °C; (e) 291 °C; (f) 300 °C; (g) afte 2 min at 300 °C; (h) fast cooling (ca. −130 °C/min) to 227 °C; (i) 199 °C; (j) 51 °C.

small nematic subdomains also with fuzzy boundaries (Figure 2e, taken at ca. 291 °C). Upon further increase in temperature to 300 °C (Figure 2f), the matrix/domain and domain/subdomain boundaries became clear; meanwhile, nearby regions of lower brightness approached and then joined the isotropic domain, where the nematic subdomains coalesced into larger droplets (5−10 μm in diameter) and gradually drifted toward and then merged with the nematic matrix. After 2 min at 300 °C, the large isotropic domain became fairly clean and almost (but not entirely) free of entrapped nematic droplets (Figure 2g). Upon fast cooling (at ca. −130 °C/min) to room temperature, the isotropic phase crystallized quickly within the temperature range of 230−200 °C, i.e., within 10 s (Figure 2h,i). The 2-min treatment at 300 °C appeared to have stabilized the phase morphology in the sense that the volume fraction of the isotropic phase remained approximately constant at ca. 40% (Figure 2j) and did not show further changes upon reheating.

**Routine DSC Analysis.** Shown in Figure 3 are the heating thermograms of a sample after an RTEP treatment and a subsequent annealing at different temperatures ($T_a$ = 100 or 150 °C) for 90 min. Annealing at

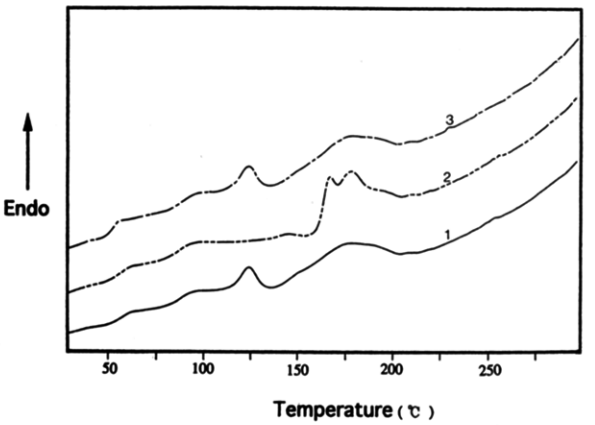


**Figure 3.** Heating thermograms after various thermal treatments: curve 1, routine thermal erasing procedure (RTEP, 2 min at 300 °C) + 90 min at 100 °C; curve 2, RTEP + 90 min at 150 °C after curve 1; curve 3, RTEP + 90 min at 100 °C after curve 2.

100 °C resulted in a melting peak in the vicinity of 120 °C, in addition to the broad melting endotherm ranging from 130 to 210 °C (curve 1). The subsequent increase of $T_a$ to 150 °C (after another RTEP treatment) squeezed the melting endotherm to the high-temperature side, covering a narrower range of 160−210 °C (curve 2), and exhibited a clear doublet sueprimposed on the broad endotherm. This was followed by a third RTEP treatment and the same sample was then annealed again at 100 °C, resulting in a reheating thermogram (curve 3) nearly the same as that after the first annealing (curve 1). It is therefore clear that the RTEP adopted here is reasonably effective in erasing the previous thermal history and affects insignificantly the general crystallization and melting behavior of the sample. Additional observations indicated that the formation of the doublet melting endotherm occurs at $T_a$ = 150 or 175 °C but not at $T_a$ = 125 °C, implying that $T_g$ of the nematic phase is within the range of 125−150 °C. This, along with results of more detailed study of annealing effects, will be the subject of a later publication since they are of no direct relevance to the present theme.

Interestingly, all three DSC traces indicated two $T_g$'s located at ca. 55 and 85 °C. The latter is in reasonable agreement with the commonly accepted $T_g$ value for the ET-rich phase in POBET. The former is simply too low to be assigned to the OB-rich phase for which $T_g$ is expected to be much higher (and therefore covered up by the broad melting endotherm) as discussed above but is in better agreement with the lower, second $T_g$ value (ca. 64 °C) reported by Gedde et al. in their dielectric measurements. It can be further noted that this lower $T_g$ grows sharper (and tends to shift slightly to lower temperatures) with increasing complexity in thermal history (cf. Figure 3). The intensification of the transition and yet lowering of the transition temperature cannot be attributed to the isothermal crystallization at 100 or 150 °C (since it is well-known that crystallization tends to suppress the intensity of the glass transition and to increase $T_g$ in semicrystalline polymers) and is more likely a result of the RTEP treatment at 300 °C as to be discussed later.

Given in Figure 4 are heating thermograms of a normal sample and the macroscopic isotropic sample (cf. the Experimental Section) after an RTEP and the subsequent fast cooling (using the liquid nitrogen cooling accessories) to −50 °C. Within the temperature range of present interest (i.e., below 100 °C), two $T_g$'s

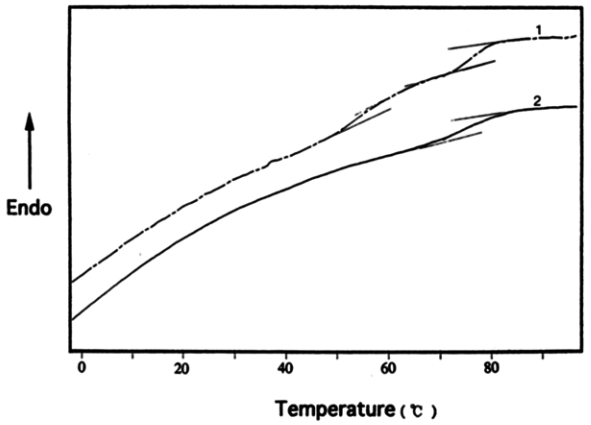


**Figure 4.** Heating thermograms after fast cooling to −50 °C from 300 °C: curve 1, a "normal" sample; curve 2, a large particle of the isotropic phase.

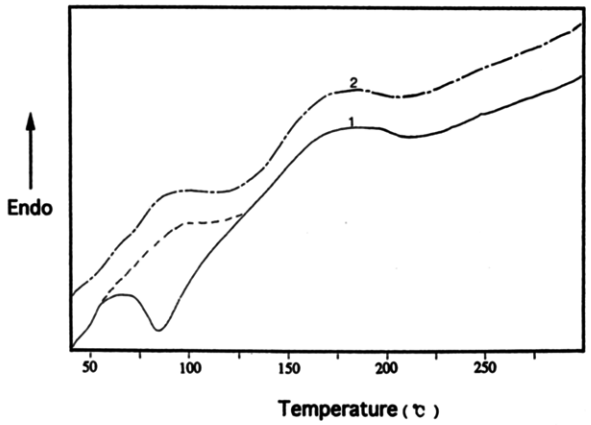


**Figure 5.** Heating thermogram (curve 1) of a sample quenched (by throwing the sample into liquid nitrogen) from 300 °C and that (curve 2) of the same sample fast-cooled (at ca. −130 °C/min) from 300 °C.

(located at ca. 80 and 55 °C, respectively) are clearly identifiable for the normal sample but there is only one $T_g$ near 80 °C for the macroscopic isotropic sample. The slight decrease in the value of the upper $T_g$ is probably attributable to the lower crystallinity in this case of more efficient cooling by use of liquid nitrogen vapor. These observations indicate clearly that the higher $T_g$ near 85 °C corresponds to the isotropic phase (hereafter abbreviated as the I-phase) typically observed via PLM. In addition, it now appears reasonable to assume that the lower-$T_g$ phase (hereafter designated as the I′-phase), although unidentifiable at the resolution of PLM, is embedded within the nematic phase zone.

**Crystallization during Reheating of a Quenched Sample.** Shown in Figure 5 are the reheating thermograms of a sample quenched (by throwing the sample into a cup of liquid nitrogen) from 300 °C and that of the same sample using the normal fast cooling after RTEP. The difference in cooling rate is clearly reflected in the presence of a crystallization exotherm ranging from 60 to 130 °C for the liquid nitrogen quenched case. Parallel PLM observations under the same temperature program indicated that the isotropic phase (which was amorphous, in contrast to the earlier case of fast cooling) in the quenched sample did not crystallize within this temperature range. Noting that the crystallization exotherm starts at ca. 60 °C (which is slightly above the lower $T_g$ of 55 °C but definitely below the second $T_g$ at 80 °C), we conclude that the exotherm corresponds to the I′-phase with $T_g$ = 55 °C.

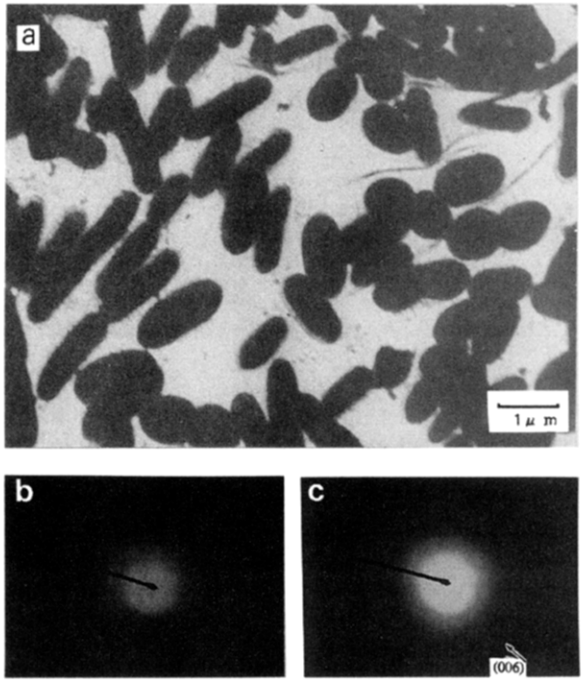


**Figure 6.** Transmission electron micrographs showing (a) the presence of I′-microdomains in the nematic matrix, (b) the SAD pattern of the I′-microdomains, and (c) the SAD pattern of the nematic matrix.

**TEM Observation.** The notion that there are I′-microdomains embedded in the nematic phase zone was supported by TEM observation of the nematic phase zone in the fast-cooled AT specimens, as shown in Figure 6. The I′-microdomains are preferentially stained by ruthenium, indicating that they are ET-rich. This is consistent with results of selected-area diffraction (SAD), which indicate PET-like features for the I′-microdomains and a POB-like pattern for the nematic matrix. The diffraction rings are low in intensity (due to low crystallinity as a result of fast cooling) and exhibit no preferred orientation (reflecting the absence of shear-induced alignment of molecular axes as a result of our experimental precaution). In addition, these microdomains are rather slender, ellipsoidal in shape. The lack of orientation (as indicated by the SAD patterns and the fairly random arrangement of the ellipsoids) suggests that the slenderness of the I′-microdomains is not an artifact due to deformation during sample preparation.

## Discussion

**Morphology Development during the First Heating.** The observation that gross morphological features of the AO sample underwent dramatic change during the first heating at a relatively high heating rate (80 °C) deserves some comments. The possibility of any direct involvement of transesterification reaction can be safely eliminated considering the relatively short period of time (ca. 3 min) involved and the fact that the sample had previously been at 275 °C for 3 h during the synthesis stage. It is clear that phase mobility is required in the development of the final phase morphology since morphological changes occurred only above ca. 200 °C (and especially above 250 °C). Noting that there are hints for the existence of the I-phase hidden in the nematic background at low temperatures (as regions of lower brightness in Figure 2b), it appears that the apparent surge of the large I-domains is through coa-

lesence of smaller droplets dispersed in the nematic phase (presumably due to the shear action during the synthesis process). The dramatic morphological evolution is therefore attributable to a purely physical process of phase coarsening and domain coalescence.

**Biphasic Nature in POBET.** Laus et al.[15] observed that the width of the molecular weight distribution (MWD) may significantly affect the biphasic gap in a main-chain liquid-crystalline polymer. Considering that a segment at the chain end can be of different free energy than those within the chain, Semenov[16] made a theoretical analysis on the fractionation effect within the biphasic gap for chains of fixed polydispersity. More recently, the effect of transesterification on MWD and hence on the phase separation is analyzed by Bladon et al.[17] based on wormlike chains with a Maier–Saupe nematic mean field. This point of view, however, cannot explain the NMR observations of Nicely et al.[8] that compositions of the isotropic and nematic phases are respectively ca. 35 and 80 mol % OB, nearly independent of the bulk composition.

Alternatively, it has been previously proposed[4] that the biphasic nature of POBET could be originated from the nonrandomness in sequence distribution. However, the NMR results of Nicely et al.[8] indicated that the nonrandomness in their POBET samples is only moderate: a "preference factor" of $m$ = ca. 1.3 was estimated. (The preference factor represents the bias in the formation of OB diads; for ideally random sequence distribution, $m = 1$.) Following the method of Nicely et al.,[8] we have determined that $m$ = ca. 1.1 for all three samples here (cf. Table 1), suggesting again only insignificant deviations from complete randomness.

Although phase separation may occur from purely geometrical (and hence entropic) consideration, the compositions of the resulting coexisting isotropic and nematic phases in this case should not be greatly different as implied in the classical work of Flory.[19] The observation of Nicely et al.[8] that compositions of the isotropic and nematic phases are significantly different (i.e., ca. 35 and 80 mol % OB, respectively) leads to the possibility that the biphasic nature here is basically originated from the unfavorable OB–ET interaction. As has been discussed previously[20–24] for random copolymers of different constituent monomers and compositions, the effective Flory–Huggins interaction parameter ($\chi_{12}$) between random copolymers 1 and 2 is related to the difference in composition as well as the pair interactions among the component segments. Consider the simplified situation of two copolymers of the same constituent monomers (A and B) but different compositions ($\phi_{iA} + \phi_{iB} = 1$ with $i = 1$ or 2, where $\phi$ denotes segmental fraction), the effective interaction parameter can be expressed as

$$\chi_{12} = \chi_{AB}(\phi_{1A} - \phi_{2A})^2 \quad (1)$$

For the case of strongly unfavorable interaction, i.e., when $\chi_{AB}$ is large and positive, it is clear that $\chi_{12}$ can be nonvanishing as long as $\phi_{1A} \neq \phi_{2A}$, which is certainly true in the present case of POBET. The unfavorable interaction between OB and ET units is understandably due to structural dissimilarity or, more specifically, due to the presence of the aliphatic ethylene linkage in the ET unit. The fact that wholly aromatic random copolyesters such as poly(*p*-oxybenzoate-*co*-2,6-naphthoate) are homogeneous[25] also lends support to the present attribution of phase separation in POBET to unfavorable segmental interaction.

In view of the general stability of phase morphology at 300 °C where the ester-exchange reaction is known to be fast,[26–29] transesterification appears important mainly within each phase (as to be further discussed later); effects of exchange reactions in the interfacial region are unlikely to be significant here. In other words, once the system is phase separated, the biphasic nature persists. With PET homopolymer as one of the starting materials, it is not exactly surprising that phase separation occurs during the synthesis process.

**Origin of the I′-Microdomains.** The presence of the I′-phase, which is ET-rich, of a rather low $T_g$ value, ellipsoidal in shape, and appears to become more fully developed during repeated RTEP treatments, poses some interesting questions. In the first place, the $T_g$ value fo 55 °C is unreasonably low considering that $T_g$ values of PET and POB are ca. 80 and 180 °C, respectively. In addition, compared to the fast coalescence of I-domains, these I′-microdomains are exceptionally resistant to coalescence, suggesting a relatively low interfacial tension as also implied by the slenderness of these I′-microdomains. These observations lead us to postulate that the I′-phase is composed of low molecular weight, ET-rich chains.

The observation of further development of the I′-microdomains implies further that this "delayed" phase-separation process is related to ester-exchange reactions. It is known that transesterification is significant[26–29] above 230 °C and therefore should be rather efficient at the temperature of RTEP treatment, i.e., 300 °C, especially in the presence of the antimony catalyst. The formation of ET-rich chains from an ET-poor matrix is more likely to occur when the site of ester exchange is in the vicinity of chain ends; exchange reactions occurring at ester linkages distance from the chain ends result in relatively long chains which are statistically unlikely to be significantly different in composition from the mean. The ET-rich chain must therefore be necessarily short, consistent with our postulation. The transesterification in the ET-rich I-phase should also result in short OB-rich chains; one might then expect the formation of nematic microdomains which mirrors the precipitation of I′-microdomains from the N-phase. This, however, was not experimentally observed. The lack of "symmetry" in the present case may be explained in terms of the greater tolerance of coils toward rods as compared to the reversed situation.[30]

**Slenderness of I′-Microdomains.** As discussed earlier, the ellipsoidal shape and the resistance to coalescence of the I′-microdomains are certainly indicative of the low interfacial tension involved. On the other hand, the interfacial tension, although admittedly low, should still tend to result in spherical domains. Hence there must be additional factors contributing to the ellipsoidal shape of the I′-domains. One possible source of the perturbation is the anisotropic nature of the nematic matrix. Due to the small size (≤ca. 1 μm) of the I′-microdomains, the director field around a hypothetical sphere of the I′-phase would be perturbed significantly in order to accommodate the curvature of the interface. This could result in unfavorable distortions (such as splaying or bending)[31,32] of the director field in the nematic phase. Since the I′-phase is easily deformable at elevated temperatures in view of the low viscosity and the low interfacial tension, the director field of the liquid-crystalline domains in contact with an I′-microdomain would tend to deform the interface (to avoid excessive increase in distortion free energy

within the nematic phase near the N/I′ interface) such that the I′-droplet is "elongated" by the director field. The key here should be the wrestling among the distortion elastic constants of the nematic phase and the interfacial tension to accommodate the spatial packing of semirigid chains near the interface. A more extensive TEM investigation is in progress, from which we hope more illuminating evidence may emerge.

## Conclusions

Glass transitions located at ca. 55 and 85 °C, respectively, were identified using DSC for a POBET material containing ca. 55 mol % OB. The higher $T_g$ was related to the large ET-rich isotropic particles typically observed via PLM. The lower $T_g$ was attributed to ET-rich microdomains within the continuous nematic phase, which were more fully developed after repeated thermal treatment at 300 °C. Existence of this low-$T_g$, ET-rich microdomain, as confirmed by TEM observations, was explained in terms of precipitation of short ET-rich chains (presumably resulting from transesterification at high temperatures) from the OB-rich nematic phase.

**Acknowledgment.** Thanks are due to Mr. Chia-Ting Chung at IMSE for his help in the PLM study. Thanks are also due to Profs. D. Gan and K. Y. Hsieh at IMSE, who recovered this manuscript file from the dying hard disk and revived the old MacIntosh SE/30 for A.C.S. This work is financially supported in part by the National Science Council, R.O.C., under Contract No. NSC84-2216-E110-007.

## References and Notes

(1) Jackson, W. L., Jr.; Kuhfuss, H. F. *J. Polym. Sci., Polym. Chem. Ed.* **1976**, *14*, 2043.
(2) Meesiri, W.; Menczel, J.; Gaur, U.; Wunderlich, B. *J. Polym. Sci., Polym. Phys. Ed.* **1982**, *20*, 719.
(3) Viney, C.; Windle, A. H. *J. Mater. Sci.* **1982**, *17*, 2661.
(4) Joseph, E.; Wilkes, G. L.; Baird, D. G. *Polymer* **1985**, *26*, 689.
(5) Takase, Y.; Mitchell, G. R.; Odajima, A. *Polym. Commun.* **1986**, *27*, 76.
(6) Cuculo, J. A.; Chen, G.-Y. *J. Polym. Sci., Polym. Phys. Ed.* **1988**, *26*, 179.
(7) Sun, T.; Porter, R. S. *Polym. Commun.* **1990**, *31*, 70.
(8) Nicely, V. A.; Dougherty, J. T.; Renfro, L. W. *Macromolecules* **1987**, *20*, 573.
(9) Gedde, U. W.; Buerger, D.; Boyd, R. H. *Macromolecules* **1987**, *20*, 988.
(10) Coburn, J. C.; Boyd, R. H. *Macromolecules* **1986**, *19*, 2238.
(11) Benson, R. S.; Lewis, D. N. *Polym. Commun.* **1987**, *28*, 289.
(12) Zachariades, A. E.; Economy, J.; Logan, J. A. *J. Appl. Polym. Sci.* **1982**, *27*, 2009.
(13) Lenz, R. W.; Jin, J.-I.; Feichtinger, K. A. *Polymer* **1983**, *24*, 327.
(14) Hedmark, P. G.; Werner, P.-E.; Westdahl, M.; Gedde, U. W. *Polymer* **1989**, *30*, 2068.
(15) Laus, M.; Caretti, D.; Angeloni, A. S.; Galli, G.; Chiellini, E. *Macromolecules* **1991**, *24*, 1459.
(16) Semenov, A. N. *Europhys. Lett.* **1993**, *21*, 37.
(17) Bladon, P.; Warner, M.; Cates, M. E. *Macromolecules* **1993**, *26*, 4499.
(18) Trent, J. S. *Macromolecules* **1984**, *17*, 2930.
(19) Flory, P. J. *Proc. R. Soc. London* **1956**, *A234*, 73.
(20) Krause, S.; Smith, A. L.; Duden, M. G. *J. Phys. Chem.* **1965**, *43*, 2144.
(21) Roe, R. J.; Zin, W. C. *Macromolecules* **1980**, *13*, 1221.
(22) Kambour, R. P.; Bendler, J. J.; Bopp, R. C. *Macromolecules* **1983**, *16*, 753.
(23) ten Brinke, G.; Karasz, F. E.; MacKnight, W. J. *Macromolecules* **1983**, *16*, 1827.
(24) Su, A. C.; Fried, J. R. *Polym. Eng. Sci.* **1987**, *27*, 1657.
(25) Economy, J.; Johnson, R. D.; Lyerla, J. R.; Muhlebach, A. In *Liquid Crystalline Polymers*; Weiss, R. A., Ober, C. K., Eds.; American Chemical Society: Washington, DC, 1990; p 129.
(26) Olbrich, E.; Chen, D.; Zachmann, H. G.; Lindner, P. *Macromolecules* **1991**, *24*, 4364.
(27) Jin, J. I. In *Liquid Crystalline Polymers*; Weiss, R. A., Ober, C. K., Eds.; American Chemical Society: Washington, DC, 1990; p 33.
(28) Arrighi, V.; Higgins, J.; Weiss, R. A.; Cimecioglu, A. L. *Macromolecules* **1992**, *25*, 5297.
(29) Li, M. H.; Brulet, A.; Keller, P.; Strazielle, C.; Cotton, J. P. *Macromolecules* **1993**, *26*, 119.
(30) Flory, P. J. *Macromolecules* **1978**, *11*, 1138.
(31) Donald, A. M.; Windle, A. H. *Liquid Crystalline Polymers*; Cambridge University Press: Cambridge, U.K., 1992.
(32) de Gennes, P. G.; Prost, J. *The Physics of Liquid Crystals*, 2nd ed.; Oxford University Press: New York, 1993.

MA946376C